Composites

Chia-Wei Wang
Ann Marie Sastry
University of Michigan, Ann Arbor, Michigan, U.S.A.

INTRODUCTION

Composite materials can be generally defined as those materials having two or more distinct material phases. With the advent of advanced polymeric composite materials, the term composite became somewhat synonymous with engineered carbon-epoxy, Kevlar-epoxy or ceramic- or metal-matrix composites, though this term later came to refer to a broader set of materials; more recently, the descriptor heterogeneous has been used to characterize study of such materials. Porous materials may also be considered composite materials, with one phase composed of void or air spaces. Examples of composites include the familiar carbon-epoxy airframe skins, and glass/epoxy or glass/polyester structural materials, e.g., helicopter rotor blades, or even furniture. Sporting goods, e.g., golf clubs, tennis rackets, and skis are also often ~~often~~ constructed of advanced composites. Even wood, which contains reinforcing cellulose fibers, bone, which may be considered a porous reinforcement, at a smaller scale, extracellular matrices, reinforced by structural proteins such as collagen, that are surrounded by ground substance (Fig. 1) constitute composites. There is a large body of literature available on both properties[1–5] and manufacturing[6] of many types of engineered composite materials, and much of this work has found, and will continue to find application in improved understanding of heterogeneous biomaterials and design of biocompatible materials.[7] As an example, of the 20–30% of the human body that is composed of proteins, up to 50% is collagen;[8] collagen's precursors have been on the planet nearly as long as multicellular life.[9] Undoubtedly, the need for improved micro and nanoscale models for the behavior of such critically important fibrous biomaterials will continue, and will support new insights into biochemistry and evolutionary science.

HISTORICAL BACKGROUND

General modeling of the properties of heterogeneous materials is of great importance to almost all engineering and scientific disciplines, and can be traced to the mid-19th century (Table 1), in work on properties of gases.[10–53] Closed-form solutions for effective properties in gases led to similar analyses for conductivity and stiffness in composite solids. Determination of engineering properties, from conductivity to stiffness, was classically accomplished via solution of Laplace's equation, whose linearizing field assumption allows simultaneous solution of a number of important problems using the same partial differential equations, rescaled using appropriate material constants (Tables 2 and 3, following the description in Ref. [54]). Other techniques that have been widely used to determine, or bound, properties of heterogeneous materials, include solutions of stress fields in representative volume elements (RVEs), models of anisotropic sheets, and models of continuum anisotropic phases. In this article, we do not attempt to survey each of these areas thoroughly; we aim, however, to give an overview of approaches in modeling composite materials, with specific results of classic models, and an eye toward the modeling of biological materials. Thus, we omit discussion of manufacture of composite materials (see, for example, Refs. [6,55,56]). Instead, we emphasize analysis of elastic and transport properties, both for their common roots in the literature, and also their importance in study of biomaterials. We begin with general formulations of anisotropic elasticity, and discuss simplifications for layered structures, which are abundant both in engineered and biological materials. Bounds on elastic properties are also discussed, since they allow estimation of material response (important in analysis of damage and growth modeling of bone, skin, and other tissues). And, a discussion of the role of phase geometry and percolation, relative to transport properties, is presented for its usefulness in estimation of both mechanical response and permeability of specific phases (e.g., structural proteins) in biomaterials.

CONTINUUM AND MICROMECHANICS OF COMPOSITE MATERIALS

Composite materials may be isotropic or anisotropic, depending on the shapes, locations, and relative sizes of the material phases. Many particulate, porous, or short-

Encyclopedia of Biomaterials and Biomedical Engineering
DOI: 10.1081/E-EBBE 120007272

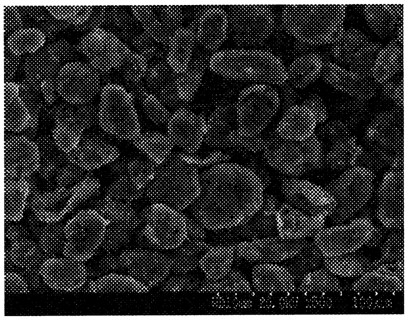

(a)

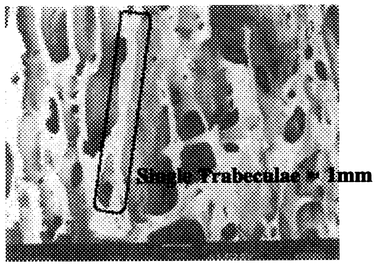

(b)

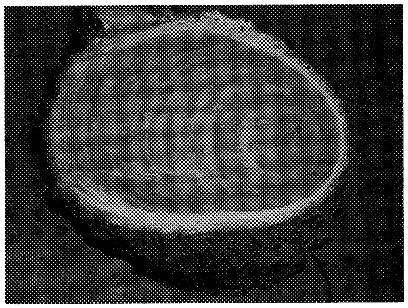

(c)

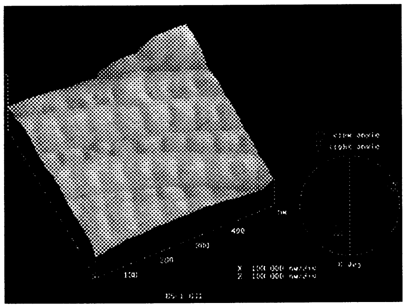

(d)

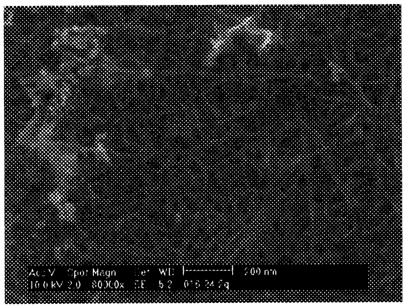

(e)

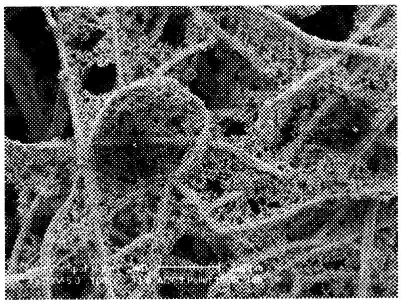

(f)

Fig. 1 Examples of composite materials, including (a) an anode of a Li-ion battery, containing carbon particles and polymeric binder, (b) trabecular bone (courtesy Dr. Scott Hollister, University of Michigan), (c) wood of an elm tree, and (d) collagen fibrils of the rat sciatic nerve perineurium, (e) carbon nanotube sheet, and (f) substrate of NiMH electrode. (*View this art in color at www.dekker.com.*)

fiber systems, for example, exhibit isotropic stiffness and conductivity; long-fiber and fabric-reinforced systems generally exhibit some degree of anisotropy.

Broadly, analysis of composite materials can be divided into two categories. Work that incorporates anisotropy into material models without detailed modeling of each phase is termed continuum mechanics, and can be used to predict effective properties of a heterogeneous material (see Ref. [57] for example). Work that directly models the shapes, locations, and relative sizes of model phases in a material is termed micromechanics, and more recently, nanomechanics, though the latter properly includes atomistic or molecular dynamics modeling and often is applied only to very small volumes due to its inherent computational intensiveness. Micromechanics is generally used to determine the details of stress, current, or other distributions (Table 2) within a heterogeneous material, along with effective properties (e.g., Refs. [1,58]). The units of the common parameters used in the deriviation of effective properties and their governing equations are listed in Table 3 and Table 4. Though theories for failure of material have been developed using continuum mechanics,[59,60] understanding of specific failure mechanisms often requires analysis of the load sharing among the constituent materials, especially for brittle reinforcements. Statistical approaches have been

Table 1 Contributions to heterogeneous mechanics, including work in disperse gases

Disperse gases		Dielectrics		Disperse media	
1850	*O.F. Mossotti*	*1955*	*W.F. Brown Jr.*	**1972**	**W.B. Russel and A. Acrivos**
1879	*R. Clausius*	**1956**	**J.D. Eshelby**	**1973**	**W.B. Russel**
1880	*L.V. Lorenz*	*1956*	*E.H. Kerner*	*1975*	*K.S. Mendelson*
1880	*H.A. Lorentz*	**1957**	**J.D. Eshelby**	1978	W.T. Doyle
1891	J.C. Maxwell	*1958*	*E. Kroner*	**1978**	**R.C. McPhedran and D.R. McKenzie**
1892	J.W. Rayleigh	**1958**	**C. van der Pol**	1978	R. Landauer
1906	*A. Einstein*	1960	R.E. Meredith and C.W. Tobias	1979	W.T. Perrins, McPhedran, and McKenzie
1912	*O. Wiener*	**1962**	**Z. Hashin**	**1979**	**R.M. Christensen and K.H. Lo**
1924	*H. Fricke*	**1962**	**Z. Hashin and S. Shtrikman**	*1988*	*D.S. McLachlan*
1924	*K. Lichtenecker*	*1964*	*J.B. Keller*	*1990*	*K.D. Bao, J. Axell, and G. Grimvall*
1925	I.Z. Runge	**1964**	**Z. Hashin and B.W. Rosen**	**1990**	**J.M. Gudes and N. Kikuchi**
1933	J.N. Goodier	**1964**	**R. Hill**	**1991**	**G.Q. Gu and Z.R. Liu**
1935	D.A.G. Bruggeman	**1965**	**R. Hill**	**1993**	**G.Q. Gu**
1947	*J.M. Dewey*	**1965**	**B. Budiansky**	**1993**	**R.M. Christensen**
1952	R. Landauer	**1966**	**Z. Hashin**	**1995**	**S.Y. Lu**
1954	*A.V. Hershey*				

Gases are in italics, conductivity of solids are in normal type, and mechanics of solids are in bold. (Adapted from Ref. [54].)

shown to be useful in developing scaling rules for failure (e.g., Refs. [61–65]). The subject of failure of heterogeneous materials is quite broad and spans modeling of ductile failure, fracture, fatigue, and creep, to name a few key phenomena. Here, we introduce modeling of constitutive properties of elastic, heterogeneous materials, from

Table 2 Effective medium theories and solution using Laplace's equation

Linear problem of interest for a two-phase material	Quantity represented by q	Quantity represented by E $E_j = U_{,j}$	Transport coefficient K	Local differential equation satisfied in each phase (in steady state)
Thermal conduction	Heat flux	Temperature gradient	Thermal conductivity	$q_i = K_{ij}E_j = K_{ij}U_{,j}$
Electrical conduction	Electric current	Electric field intensity	Electrical conductivity	$\nabla \cdot \vec{q} = 0$
Electrical insulation	Electric displacement	Electric field intensity	Dielectric constant	
Permeation of a porous medium consisting of a fixed array of small rigid particles with an incompressible Newtonian fluid	Force on particles in unit volume of mixture (=pressure gradient calculated from pressure drop between distant parallel planes)	Flux of fluid volume relative to particles	Permeability (Darcy constant divided by μ)	$\nabla p = \mu\nabla^2\vec{u}$ $\nabla \cdot \vec{u} = 0$ where $\vec{u}$=velocity; p=pressure; μ=viscosity
Elasticity of a medium containing elastic inclusions embedded in an elastic matrix	Stress	Strain	Lame constants (or rigidity and bulk moduli)	$\vec{q} = 2\mu\vec{E} + \lambda\vec{E}I$ $\nabla \cdot \vec{q} = 0$ μ, λ=local Lame constants

(Adapted from Ref. [54].)

Table 3 Common units for conversion of parameters in Table 2

	q	U	E	K
Thermal conduction	J/m^2	K (temperature)	K/m	$J/m \cdot K$
Electrical conduction	Amp/m^2	V	V/m	S/m
Electrical insulation	C/m^2	V	V/m	f/m
Porous medium	m/s	m	1	m/s
Elasticity	F/m^2	m	1	F/m^2

the continuum to microscale, and comment on applications for both constitutive and failure modeling.

CONTINUUM, ANISOTROPIC STIFFNESS

The number of stiffnesses required to fully characterize a material's response depends upon the degree of its anisotropy. Counterintuitively, tensorial stiffnesses are denoted C_{ijkl}, and tensorial compliances are denoted S_{ijkl}. An elastic constitutive relation (using the notation of Fig. 2) can be expressed as either

$$\sigma_{ij} = C_{ijkl}\varepsilon_{kl} \tag{1}$$

or

$$\varepsilon_{ij} = S_{ijkl}\sigma_{kl} \tag{2}$$

respectively, where ε_{kl} is the infinitesimal strain tensor and σ_{ij} is the stress tensor. We note that 2-D sections of the internal structure of a composite material depend on the plane examined, but models using 3-D ellipsoidal or cylindrical inclusions can be used to represent a wide range of reinforcement shapes (Fig. 3), from particles (2-D circles or ellipses, or 3-D spheres or ellipsoids) to fibers (1-D lines, 2-D ellipses or circles, or 3-D cylinders or ellipsoids).

The number of nonzero components of the stiffness tensor and the relationships among its components can be determined using material symmetry and equilibrium considerations. As a first cut, the 81 coefficients in the

Table 4 Common governing equations for modeling physical phenomena

Equation	Formula	Phenomena	Solution
Wave	$\nabla^2\mathbf{V} = \kappa\dfrac{\partial\mathbf{V}}{\partial t}$	1. Wave	1. Analytical solution by various transformations, e.g. Bäcklund transformation, Green's function, integral transform, Lax Pair, separation of variables 2. Numerical solution, e.g. finite element method
Diffusion	$\dfrac{\partial\mathbf{V}}{\partial t} = \kappa\nabla^2\mathbf{V}$	1. Heat conduction 2. Mass diffusion	1. Analytical solution by separation of variables, Laplace transform, Fourier transform, Green's function 2. Numerical solution, e.g. finite element method
Poisson	$\nabla^2\mathbf{V} = -4\pi\rho$	1. Electrostatics with constant source or sink 2. Thermal field with constant source or sink	1. Analytical solution by separation of variables, 2. Numerical solution, e.g. finite element method
Laplace	$\nabla^2\mathbf{V} = 0$	1. Thermal conduction 2. Electrostatics 3. Incompressible fluid flow 4. Membrane mechanics 5. Elasticity	1. Analytical solution by separation of variables. 2. Numerical solution, e.g. finite element method

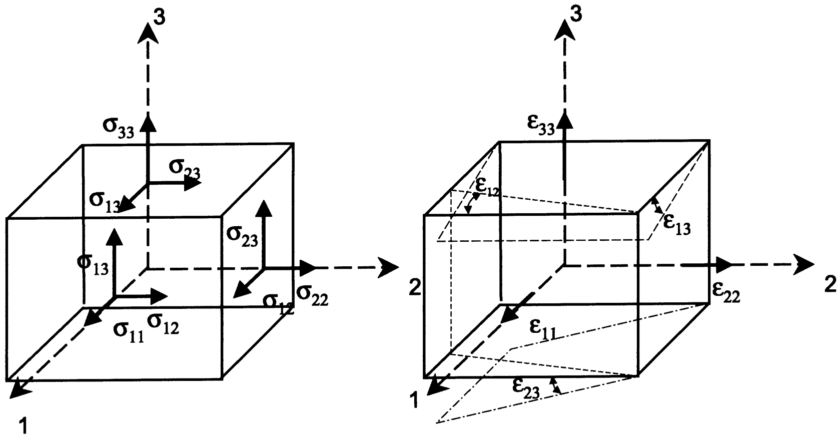

Fig. 2 Coordinate axes and components for the stress and strain tensors in 3D.

C_{ijkl} tensor can be seen immediately to have only 36 independent coefficients due to the symmetry of σ_{ij} and ε_{kl}, as

$$\sigma_{ij} = \sigma_{ji} \text{ and } \varepsilon_{kl} = \varepsilon_{lk}$$

We can then write the constitutive rule in matrix form (e.g., Refs. [66,67] for notation and general methods that follow) as

$$\begin{bmatrix} \sigma_1 \\ \sigma_2 \\ \sigma_3 \\ \sigma_4 \\ \sigma_5 \\ \sigma_6 \end{bmatrix} = \begin{bmatrix} C_{11} & C_{12} & C_{13} & C_{14} & C_{15} & C_{16} \\ C_{21} & C_{22} & C_{23} & C_{24} & C_{25} & C_{26} \\ C_{31} & C_{32} & C_{33} & C_{34} & C_{35} & C_{36} \\ C_{41} & C_{42} & C_{43} & C_{44} & C_{45} & C_{46} \\ C_{51} & C_{52} & C_{53} & C_{54} & C_{55} & C_{56} \\ C_{61} & C_{62} & C_{63} & C_{64} & C_{65} & C_{66} \end{bmatrix} \begin{bmatrix} \varepsilon_1 \\ \varepsilon_2 \\ \varepsilon_3 \\ \varepsilon_4 \\ \varepsilon_5 \\ \varepsilon_6 \end{bmatrix} \tag{3}$$

where C_{ij} are the elastic stiffness coefficients, and

$$\begin{aligned} \sigma_1 &= \sigma_{11}; \sigma_2 = \sigma_{22}; \sigma_3 = \sigma_{33}; \sigma_4 = \sigma_{23}; \sigma_5 \\ &= \sigma_{13}; \sigma_6 = \sigma_{12} \\ \varepsilon_1 &= \varepsilon_{11}; \varepsilon_2 = \varepsilon_{22}; \varepsilon_3 = \varepsilon_{33}; \varepsilon_4 = 2\varepsilon_{23}; \varepsilon_5 \\ &= 2\varepsilon_{13}; \varepsilon_6 = 2\varepsilon_{12} \end{aligned} \tag{4}$$

The requirement of symmetry in C_{ij} further reduces the number of independent coefficients to 21.

Further, nontrivial reductions of the stiffness tensor (i.e., for a number of independent coefficients greater than 2) can be obtained for aligned fibrous materials, wherein the transverse arrangement of fibers determines the degree of anisotropy (Fig. 4). Materials containing square-packed fibers (Fig. 4a) are termed orthotropic, since they contain at least two mutually orthogonal planes of symmetry; in this case, the number of elastic coefficients is reduced to 9, as

$$\begin{bmatrix} \sigma_1 \\ \sigma_2 \\ \sigma_3 \\ \sigma_4 \\ \sigma_5 \\ \sigma_6 \end{bmatrix} = \begin{bmatrix} C_{11} & C_{12} & C_{13} & 0 & 0 & 0 \\ C_{12} & C_{22} & C_{23} & 0 & 0 & 0 \\ C_{13} & C_{23} & C_{33} & 0 & 0 & 0 \\ 0 & 0 & 0 & C_{44} & 0 & 0 \\ 0 & 0 & 0 & 0 & C_{55} & 0 \\ 0 & 0 & 0 & 0 & 0 & C_{66} \end{bmatrix} \begin{bmatrix} \varepsilon_1 \\ \varepsilon_2 \\ \varepsilon_3 \\ \varepsilon_4 \\ \varepsilon_5 \\ \varepsilon_6 \end{bmatrix} \tag{5}$$

Materials containing aligned, hexagonally packed fibers or randomly arranged fibers (Figs. 4b and 4c) are termed transversely isotropic, since the elastic properties are invariant with respect to an arbitrary rotation about an axis parallel to the fibers' axis; in this case, the number of independent stiffness coefficients is reduced to 5, as

$$\begin{bmatrix} \sigma_1 \\ \sigma_2 \\ \sigma_3 \\ \sigma_4 \\ \sigma_5 \\ \sigma_6 \end{bmatrix} = \begin{bmatrix} C_{11} & C_{12} & C_{13} & 0 & 0 & 0 \\ C_{12} & C_{11} & C_{13} & 0 & 0 & 0 \\ C_{13} & C_{13} & C_{33} & 0 & 0 & 0 \\ 0 & 0 & 0 & C_{44} & 0 & 0 \\ 0 & 0 & 0 & 0 & C_{44} & 0 \\ 0 & 0 & 0 & 0 & 0 & \dfrac{C_{11} - C_{12}}{2} \end{bmatrix} \begin{bmatrix} \varepsilon_1 \\ \varepsilon_2 \\ \varepsilon_3 \\ \varepsilon_4 \\ \varepsilon_5 \\ \varepsilon_6 \end{bmatrix} \tag{6}$$

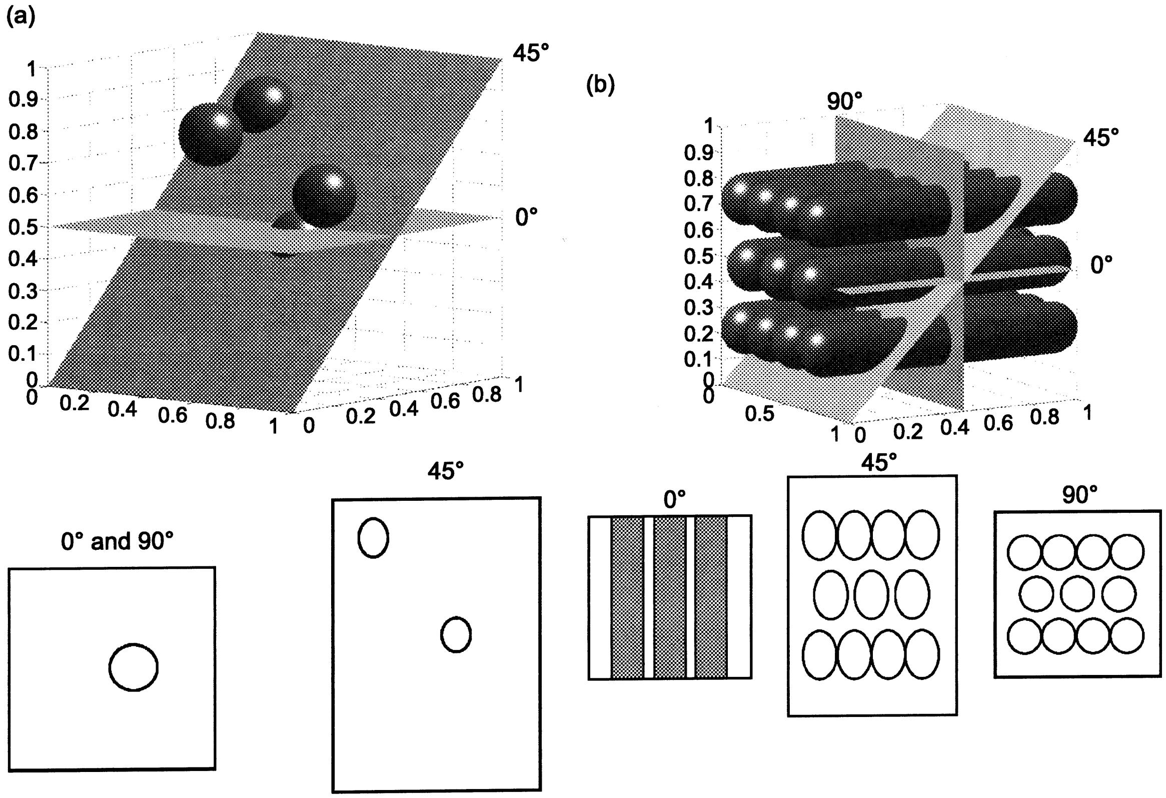

Fig. 3 Cross-sections of (a) particulate and (b) fibrous composite materials.

Composites composed of layers of fibrous sheets, or laminae, are termed laminates or laminated composites. Analysis of the elastic properties of a stack of such layers (Fig. 5) requires modeling of both the in-plane properties of each layer and an assumed for an out-of-plane displacement function for the stack. Classically, this is accomplished using the well known laminate theory, in which an elastic stiffness matrix, the ABBD matrix, is assembled for the stack. A standard notation is shown in Fig. 5; the laminate code is enclosed in brackets, with sequential plies designated by the in-plane orientation of their fibers. Subscripts s and t are used to denote sym-

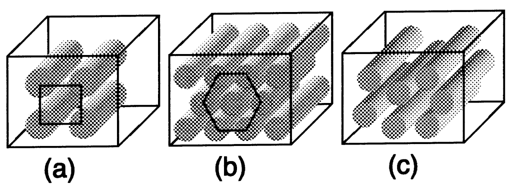

Fig. 4 Several classical transverse arrangements assumed for aligned-fiber composites, including (a) square packing, (b) hexagonal close-packing and (c) random packing.

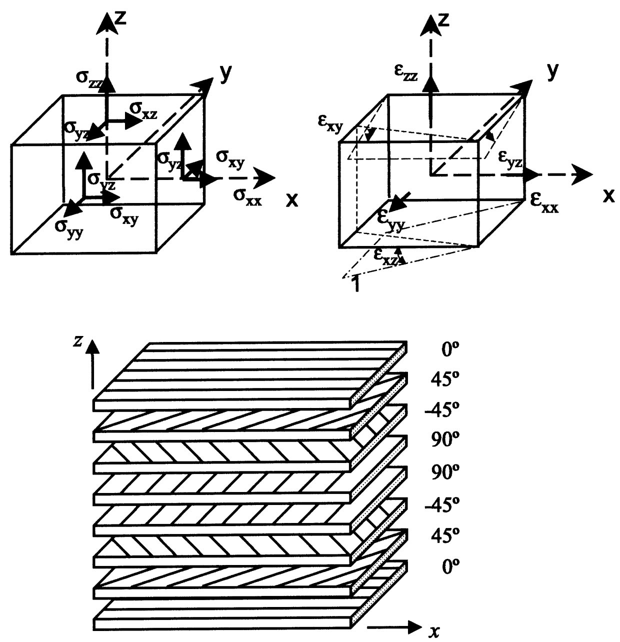

Fig. 5 Notation for laminated composites, with in-plane orientation of fibers in each layer designated in degrees. The example shown is a symmetric, quasi-isotropic laminate, $[0/\pm45/90]_s$.

metric or total, respectively. Symmetry in the orientations of the layers about the midplane prevents bend-twist coupling in the laminate, discussed later. Also, many laminates are designed to have in-plane properties that are independent of rotation (quasi-isotropy), as in the example of Fig. 5.

Plane stress is assumed in each layer. Normal stress resultants in the x direction, N_x, in the y direction, N_y, and in shear, N_{xy}, are defined as

$$N_x = \int_{-H/2}^{H/2} \sigma_x dz \qquad N_y = \int_{-H/2}^{H/2} \sigma_y dz \qquad N_{xy} = \int_{-H/2}^{H/2} \sigma_{xy} dz \tag{7}$$

and moment resultants, M_x, M_y, and M_{xy}, are defined as

$$M_x = \int_{-H/2}^{H/2} \sigma_x z dz \qquad M_y = \int_{-H/2}^{H/2} \sigma_y z dz \qquad M_{xy} = \int_{-H/2}^{H/2} \tau_{xy} z dz \tag{8}$$

The plane stress assumption (σ_3, τ_{23}, and $\tau_{13}=0$) results in the 2-D reduction of Eq. 3 to

$$\begin{bmatrix} \sigma_1 \\ \sigma_2 \\ \tau_{12} \end{bmatrix} = \begin{bmatrix} Q_{11} & Q_{12} & 0 \\ Q_{12} & Q_{22} & 0 \\ 0 & 0 & Q_{66} \end{bmatrix} \begin{bmatrix} \varepsilon_1 \\ \varepsilon_2 \\ \gamma_{12} \end{bmatrix} \tag{9}$$

where

$$\begin{aligned} Q_{11} &= C_{11} - \frac{C_{13}^2}{C_{33}} \\ Q_{12} &= C_{12} - \frac{C_{13}C_{23}}{C_{33}} \\ Q_{22} &= C_{22} - \frac{C_{23}^2}{C_{33}} \\ Q_{66} &= Q_{66} \end{aligned} \tag{10}$$

We note that for the 2-D case, these relations apply to both transversely isotropic or orthotropic laminae. Transformation of stiffnesses (Eq. 9) to a global coordinate system is required for each layer, where the transformed stiffnesses are denoted $\overline{Q}_{ij}$, as in

$$\begin{bmatrix} \sigma_x \\ \sigma_y \\ \tau_{xy} \end{bmatrix} = \begin{bmatrix} \overline{Q}_{11} & \overline{Q}_{12} & \overline{Q}_{16} \\ \overline{Q}_{12} & \overline{Q}_{22} & \overline{Q}_{26} \\ \overline{Q}_{16} & \overline{Q}_{26} & \overline{Q}_{66} \end{bmatrix} \begin{bmatrix} \varepsilon_x \\ \varepsilon_y \\ \gamma_{xy} \end{bmatrix} \tag{11}$$

and are obtained from the Q_{kl} by

$$\begin{aligned} \overline{Q}_{11} &= Q_{11}\cos^4\theta + 2(Q_{12} + 2Q_{66})\sin^2\theta\cos^2\theta \\ &\quad + Q_{22}\sin^4\theta \\ \overline{Q}_{12} &= (Q_{11} + Q_{22} - 4Q_{66})\sin^2\theta\cos^2\theta \\ &\quad + Q_{12}(\sin^4\theta + \cos^4\theta) \\ \overline{Q}_{16} &= (Q_{11} - Q_{12} - 2Q_{66})\sin\theta\cos^3\theta \\ &\quad + (Q_{12} - Q_{22} - 2Q_{66})\cos\theta\sin^3\theta \\ \overline{Q}_{22} &= Q_{11}\sin^4\theta + 2(Q_{12} + 2Q_{66})\sin^2\theta\cos^2\theta \\ &\quad + Q_{22}\cos^4\theta \\ \overline{Q}_{26} &= (Q_{11} - Q_{22} - 2Q_{66})\sin^3\theta\cos\theta \\ &\quad + (Q_{12} - Q_{22} + 2Q_{66})\sin\theta\cos^3\theta \\ \overline{Q}_{66} &= (Q_{11} + Q_{22} - 2Q_{12} - 2Q_{66})\sin^2\theta\cos^2\theta \\ &\quad + Q_{66}(\sin^4\theta + \cos^4\theta) \end{aligned} \tag{12}$$

Use of the Kirchhoff–Love hypothesis, that plane transverse sections remain plane during loading, results in

$$\begin{aligned} u &= u_o - z\frac{\partial w_o}{\partial x} \\ v &= v_o - z\frac{\partial w_o}{\partial y} \\ w &= w_o \end{aligned} \tag{13}$$

for the displacement (u, v, w) of a point at (x, y, z), given midplane displacements (u_o, v_o, w_o). The strains can then be calculated via

$$\begin{aligned} \varepsilon_x &= \frac{\partial u}{\partial x} = \frac{\partial u_o}{\partial x} - z\frac{\partial^2 w_o}{\partial x^2} = \varepsilon_x^o - z\frac{\partial^2 w_o}{\partial x^2} \\ \varepsilon_y &= \frac{\partial v}{\partial y} = \frac{\partial v_o}{\partial y} - z\frac{\partial^2 w_o}{\partial x^2} = \varepsilon_y^o - z\frac{\partial^2 w_o}{\partial x^2} \\ \gamma_{xy} &= \frac{\partial u}{\partial y} + \frac{\partial v}{\partial x} = \frac{\partial u_o}{\partial y} + \frac{\partial v_o}{\partial x} - 2z\frac{\partial^2 w_o}{\partial x \partial y} \\ &= \gamma_{xy}^o - 2z\frac{\partial^2 w_o}{\partial x \partial y} \end{aligned} \tag{14}$$

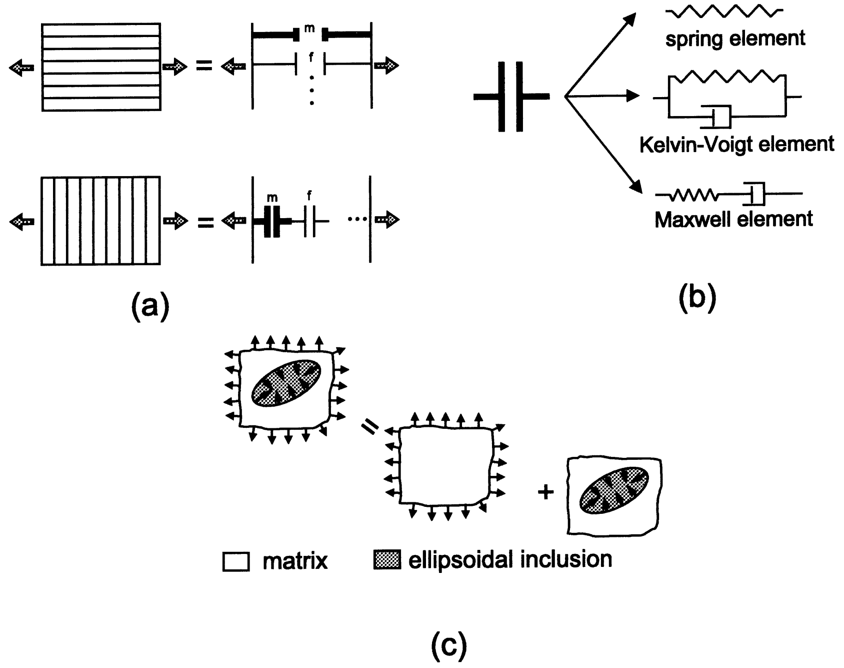

Fig. 6 Possible levels of detail in micromechanical models, from (a) simple rule of mixtures in series and parallel for stiffness modeling, (b) the element in (a) can be represent for spring, Kelvin–Voigt (spring-dashpot in parallel) element, or Maxwell (spring-dashpot in series) element, to (c) derivation of the stress fields around elliptical particles.

Assuming small rotations, displacements u and v in Eq. 13, the strains, can expressed as

$$
\begin{aligned}
\varepsilon_x &= \frac{\partial u}{\partial x} = \frac{\partial u_o}{\partial x} - z\frac{\partial^2 w_o}{\partial x^2} = \varepsilon_x^o + z\kappa_x^o \\
\varepsilon_y &= \frac{\partial v}{\partial y} = \frac{\partial v_o}{\partial y} - z\frac{\partial^2 w_o}{\partial x^2} = \varepsilon_y^o + z\kappa_y^o \\
\gamma_{xy} &= \frac{\partial u}{\partial y} + \frac{\partial v}{\partial x} = \frac{\partial u_o}{\partial y} + \frac{\partial v_o}{\partial x} - 2z\frac{\partial^2 w_o}{\partial x \partial y} \\
&= \gamma_{xy}^o + z\kappa_{xy}^o
\end{aligned}
\tag{15}
$$

and Eq. 11 can be rewritten as

$$
\begin{bmatrix} \sigma_x \\ \sigma_y \\ \tau_{xy} \end{bmatrix} = \begin{bmatrix} \overline{Q}_{11} & \overline{Q}_{12} & \overline{Q}_{16} \\ \overline{Q}_{12} & \overline{Q}_{22} & \overline{Q}_{26} \\ \overline{Q}_{16} & \overline{Q}_{26} & \overline{Q}_{66} \end{bmatrix} \begin{bmatrix} \varepsilon_x^o + z\kappa_x^o \\ \varepsilon_y^o + z\kappa_x^o \\ \gamma_{xy}^o + z\kappa_{xy}^o \end{bmatrix} \tag{16}
$$

Finally, a global stiffness matrix for both in-plane displacements and out-of-plane moments can be expressed in terms of the ABBD matrix as

$$
\begin{bmatrix} N_x \\ N_y \\ N_{xy} \end{bmatrix} = \begin{bmatrix} A_{11} & A_{12} & A_{16} \\ A_{12} & A_{22} & A_{26} \\ A_{61} & A_{26} & A_{66} \end{bmatrix} \begin{bmatrix} \varepsilon_x^o \\ \varepsilon_y^o \\ \gamma_{xy}^o \end{bmatrix} + \begin{bmatrix} B_{11} & B_{12} & B_{16} \\ B_{12} & B_{22} & B_{26} \\ B_{16} & B_{26} & B_{66} \end{bmatrix} \begin{bmatrix} \kappa_x^o \\ \kappa_y^o \\ \kappa_{xy}^o \end{bmatrix} \tag{17}
$$

$$
\begin{bmatrix} M_x \\ M_y \\ M_{xy} \end{bmatrix} = \begin{bmatrix} B_{11} & B_{12} & B_{16} \\ B_{12} & B_{22} & B_{26} \\ B_{16} & B_{26} & B_{66} \end{bmatrix} \begin{bmatrix} \varepsilon_x^o \\ \varepsilon_y^o \\ \gamma_{xy}^o \end{bmatrix} + \begin{bmatrix} D_{11} & D_{12} & D_{16} \\ D_{12} & D_{22} & D_{26} \\ D_{16} & D_{26} & D_{66} \end{bmatrix} \begin{bmatrix} \kappa_x^o \\ \kappa_y^o \\ \kappa_{xy}^o \end{bmatrix} \tag{18}
$$

where

$$A_{ij} = \int_{-H/2}^{H/2} \overline{Q}_{ij} dz \approx \sum_{k=1}^{N} \overline{Q}_{ij_k}(z_k - z_{k-1})$$

$$B_{ij} = \int_{-H/2}^{H/2} \overline{Q}_{ij} z dz \approx \sum_{k=1}^{N} \overline{Q}_{ij_k}(z_k^2 - z_{k-1}^2)$$

$$D_{ij} = \int_{-H/2}^{H/2} \overline{Q}_{ij} z^2 dz \approx \frac{1}{3} \sum_{k=1}^{N} \overline{Q}_{ij_k}(z_k^3 - z_{k-1}^3) \quad (19)$$

The matrices represent extensional stiffness (A), bending (D), and bend-twist coupling (B). If each layer of laminate is thin, the terms A_{ij}, B_{ij}, and D_{ij} can be approximated from the sums shown in Eq. 19, and we can write the laminate constitutive law as

$$\begin{bmatrix} N_x \\ N_y \\ N_{xy} \\ M_x \\ M_y \\ M_{xy} \end{bmatrix} = \begin{bmatrix} A_{11} & A_{12} & A_{16} & B_{11} & B_{12} & B_{16} \\ A_{12} & A_{22} & A_{26} & B_{12} & B_{22} & B_{26} \\ A_{16} & A_{26} & A_{66} & B_{16} & B_{26} & B_{66} \\ B_{11} & B_{12} & B_{16} & D_{11} & D_{12} & D_{16} \\ B_{12} & B_{22} & B_{26} & D_{12} & D_{22} & D_{26} \\ B_{16} & B_{26} & B_{66} & D_{16} & D_{26} & D_{66} \end{bmatrix} \begin{bmatrix} \varepsilon_x^o \\ \varepsilon_y^o \\ \gamma_{xy}^o \\ \kappa_x^o \\ \kappa_y^o \\ \kappa_{xy}^o \end{bmatrix} \quad (20)$$

We note that the dimensions of these parameters are scaled per unit length of the laminate, i.e., N_i and A_{ij} are expressed in force per unit length, M_i and B_{ij}, in force, and D_{ij} as force × length. As usual, ε is dimensionless; curvature κ is dimensioned as inverse length.

These relations have been widely implemented in free and commercially available codes, and are a cornerstone of laminate design. However, though laminate theory can satisfactorily model the behavior of the composite at the lamina or laminate scale, the details of load sharing among the constituent materials and many aspects of failure require more detailed modeling of the phases.

MICROMECHANICS OF ORDERED AND DISORDERED COMPOSITES

Micromechanical approaches take specific account of each phase in modeling. Classical approaches (Fig. 6a) span simple strength-of-materials series[68] and parallel[69] models, to early 2-D elastic field solutions for stresses around elliptical particles (e.g., Ref. [70]). All of these stemmed, along with much other work in the field, from the classical work of Eshelby.[27] To model polymeric systems having viscoelastic behavior, elements in each model can be replaced with Voigt–Kelvin (parallel spring-dashpot) or Maxwell (series spring-dashpot) elements, as illustrated in Fig. 6b. In present applications, modeling of the details of even elastic load transfer in constituent phases (with engineering fibers of O(10–100 μm)) in a simulation of structural properties (of components of O(>1 cm)) is still somewhat beyond computational capability, though detailed finite element analyses of load transfer have found great utility in informing less-detailed models of structural response and failure (e.g., Ref. [67]). Here, we emphasize the classical work in analytical elasticity (Fig. 7), employing simplifying assumptions for the shapes of the phases in composite media in order to directly perform energy and mechanics of materials analyses to derive field solutions for stresses, strains, and stiffnesses.

Though many fibers are anisotropic, especially with regard to thermal expansion (e.g., many carbon fibers have a slightly negative axial coefficient of thermal expansion and a positive transverse CTE), the classical micromechanics models view each phase as isotropic. Thus, we complete the reduction of the stiffness tensor described earlier for single, isotropic phases to (see below) for which there are only two independent components of C_{ij}. Engineering constants, such as Young's modulus E, shear modulus μ, and bulk modulus K can be readily obtained from these tensorial stiffnesses. For example, if we specify

$$\varepsilon_1 = \varepsilon_2 = \varepsilon_3 = \varepsilon \quad (22)$$

and

$$\sigma_1 = \sigma_2 = \sigma_3 = \sigma \quad (23)$$

we can find from the definition of bulk modulus K,

$$\sigma = 3K\varepsilon \quad (24)$$

$$\begin{bmatrix} \sigma_1 \\ \sigma_2 \\ \sigma_3 \\ \sigma_4 \\ \sigma_5 \\ \sigma_6 \end{bmatrix} = \begin{bmatrix} C_{11} & C_{12} & C_{12} & 0 & 0 & 0 \\ C_{12} & C_{11} & C_{12} & 0 & 0 & 0 \\ C_{12} & C_{12} & C_{11} & 0 & 0 & 0 \\ 0 & 0 & 0 & (C_{11} - C_{12}) & 0 & 0 \\ 0 & 0 & 0 & 0 & (C_{11} - C_{12}) & 0 \\ 0 & 0 & 0 & 0 & 0 & (C_{11} - C_{12}) \end{bmatrix} \begin{bmatrix} \varepsilon_1 \\ \varepsilon_2 \\ \varepsilon_3 \\ \varepsilon_4 \\ \varepsilon_5 \\ \varepsilon_6 \end{bmatrix} \quad (21)$$

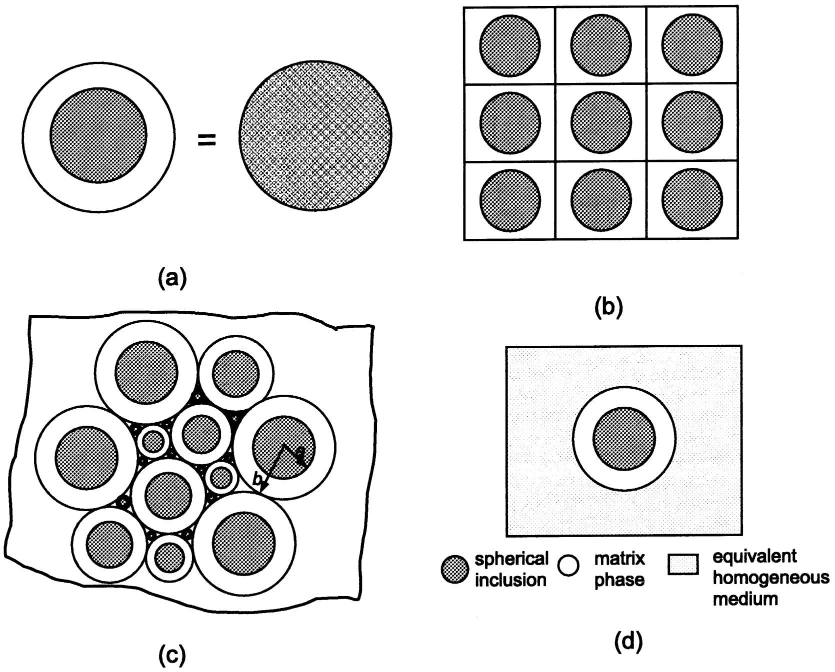

Fig. 7 Micromechanical models of ordered composite materials, including representative volume elements for the effective medium theories of (a) Maxwell's model (see Ref. [14]), (b) Rayleigh's rectangular array (see Ref. [15]), (c) Hashin's composite sphere model (see Ref. [31]) and (d) Christiansen and Lo's three phases model (see Ref. [46]).

that

$$K = \frac{1}{3}(C_{11} + 2C_{12}) \tag{25}$$

The shear moduli are defined as

$$\mu = \mu_{12} = \mu_{31} = \mu_{23} = \frac{1}{2}(C_{11} - C_{12}) \tag{26}$$

and Young's modulus and Poisson's ratio can be then determined by bulk modulus K and shear modulus μ as

$$E = \frac{9K\mu}{3K + \mu} \tag{27}$$

and

$$v = \frac{3K - 2\mu}{2(3K + \mu)} \tag{28}$$

Both somewhat realistic and purely theoretical constructs have been used to derive effective properties (both conductive and mechanical) using micromechanical analyses, and both classes of RVEs have contributed to literature on the bounding of effective properties. In the first category, wherein fibers or particles are somewhat literally represented in 2-D as circles or ellipsoids (see Fig. 3), the derivations of Maxwell[14] and Rayleigh[15] were among the first to allow calculation of effective conductive properties based on relative fraction of materials packed in a regular fashion. Later, Bruggeman analyzed both a "symmetric effective medium" and an "asymmetrical effective medium" by assuming a wide distribution for the sizes of inclusions.[22] In 1962, Hashin introduced a composite sphere model (Fig. 7c) using Eshelby's energy approach (Fig. 6b) to develop a closed-form solution for effective stiffness of a continuous matrix phase infused with a variable-diameter sphere.[31] The ratio of radii *a*/*b* for the phases was taken as a constant, proportional to the volumetric ratio of each composite sphere and independent of their absolute size.

Schemes involving theoretical material constructs have also allowed for solution of the field equations to estimate effective properties; these so-called self-consistent domains are analyzed by matching average stress and strain in the inclusion phases and the uniform stress and strain in the surrounding, infinite, isotropic medium. The first self-consistent formulations were developed by Hershey[71] and Kröner[72] in modeling polycrystalline media (Fig. 7d).

Table 5 Summary of the rigorous bounds of physical properties for transverse isotropic composites materials

Property	Lower bound	Upper bound
E_1	$E_1^L = \mathbf{v}^f E_1^f + \mathbf{v}^m E_1^m + \dfrac{4\left(v_{12}^m - v_{12}^f\right)^2 k^f k^m G_{12}^m}{\left[k^m k^f + G_{12}^m(\mathbf{v}^f k^f + \mathbf{v}^m k^m)\right]}$	$E_1^U = \mathbf{v}^f E_1^f + \mathbf{v}^m E_1^m + \dfrac{4\left(v_{12}^f - v_{12}^m\right)^2 k^f k^m G_{12}^f}{\left[k^m k^f + G_{12}^f(\mathbf{v}^f k^f + \mathbf{v}^m k^m)\right]}$
$\nu_{12}=\nu_{13}$	$v_{12}^L = v_{13}^L = \mathbf{v}^m v_{12}^m + \mathbf{v}^f v_{12}^f + \dfrac{\left(v_{12}^m - v_{12}^f\right)\left(k^f - k^m\right)}{\left[k^m k^f + G_{12}^m(\mathbf{v}^m k^m + \mathbf{v}^f k^f)\right]}$	$v_{12}^U = v_{13}^U = \mathbf{v}^m v_{12}^m + \mathbf{v}^f v_{12}^f + \dfrac{\left(v_{12}^f - v_{12}^m\right)\left(k^m - k^f\right)}{\left[k^m k^f + G_{12}^f(\mathbf{v}^m k^m + \mathbf{v}^f k^f)\right]}$
G_{12}	$G_{12}^L = \dfrac{G_{12}^m\left[\left(G_{12}^f + G_{12}^m\right) + \mathbf{v}^f\left(G_{12}^f - G_{12}^m\right)\right]}{\left[\left(G_{12}^f + G_{12}^m\right) - \mathbf{v}^f\left(G_{12}^f - G_{12}^m\right)\right]}$	$G_{12}^U = \dfrac{G_{12}^f\left[\left(G_{12}^f + G_{12}^m\right) + \mathbf{v}^m\left(G_{12}^m - G_{12}^f\right)\right]}{\left[\left(G_{12}^f + G_{12}^m\right) - \mathbf{v}^m\left(G_{12}^m - G_{12}^f\right)\right]}$
G_{23}	$G_{23}^L = \dfrac{G_{23}^m\left[k^f\left(G_{23}^f + G_{23}^m\right) + 2G_{23}^f G_{23}^m + \mathbf{v}^f k^m\left(G_{23}^f - G_{23}^m\right)\right]}{\left[k^m\left(G_{23}^f + G_{23}^m\right) + 2G_{23}^f G_{23}^m - \mathbf{v}^f\left(G_{23}^f - G_{23}^m\right)\left(k^m + 2G_{23}^m\right)\right]}$	$G_{23}^U = \dfrac{G_{23}^f\left[k^m\left(G_{23}^f + G_{23}^m\right) + 2G_{23}^f G_{23}^m + \mathbf{v}^m k^f\left(G_{23}^m - G_{23}^f\right)\right]}{\left[k^f\left(G_{23}^f + G_{23}^m\right) + 2G_{23}^f G_{23}^m - \mathbf{v}^m\left(G_{23}^m - G_{23}^f\right)\left(k^f + 2G_{23}^f\right)\right]}$
$\mathbf{k}$	$k^L = \dfrac{k^m(k^f + G_{23}^m) + \mathbf{v}^f G_{23}^m(k^f - k^m)}{\left[(k^f + G_{23}^m) - \mathbf{v}^f(k^f - k^m)\right]}$	$k^U = \dfrac{k^f\left(k^m + G_{23}^f\right) + \mathbf{v}^m G_{23}^f(k^m - k^f)}{\left[\left(k^m + G_{23}^f\right) - \mathbf{v}^m\left(k^m - k^f\right)\right]}$
$E_2=E_3$	$E_2^L = E_3^L = \dfrac{1}{\dfrac{1}{4G_{23}^L} + \dfrac{1}{4k^L} + \dfrac{(v_{12}^U)^2}{E_1^L}}$	$E_2^U = E_3^U = \dfrac{1}{\dfrac{1}{4G_{23}^U} + \dfrac{1}{4k^U} + \dfrac{(v_{12}^L)^2}{E_1^U}}$
ν_{23}	$v_{23}^L = \dfrac{2E_1^L k^L - E_1^L E_2^L - 4(v_{12}^U)^2 k^L E_2^L}{2E_1^L k^L}$	$v_{23}^U = \dfrac{2E_1^U k^U - E_1^U E_2^U - 4(v_{12}^L)^2 k^U E_2^U}{2E_1^U k^U}$

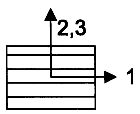

Superscripts "L" and "U" indicate lower and upper bounds, respectively, for corresponding physical properties. Superscripts "f" and "m" indicate fiber and matrix phases, respectively. All formulae adapted from Ref. [76].

Table 6 Summary of rigorous bounds physical properties for particulate-filled composite materials

Property	Lower bound	Upper bound
K	$k^L = \frac{k^m(k^f(1 + (\mathbf{v}^f)^2(2\mathbf{v}^f - 2\mathbf{v}^m) + \mathbf{v}^m) + 2k_m((\mathbf{v}^f)^2 - 1)(\mathbf{v}^m - \mathbf{v}^f))}{k^f(\mathbf{v}^m)(1 + \mathbf{v}^m) + k^m(2 + \mathbf{v}^f + (\mathbf{v}^f - 4)\mathbf{v}^m)}$	$k^U = \frac{k^f\left\{2k^f(\mathbf{v}^f)^2(\mathbf{v}^f - \mathbf{v}^m) + k^m\left[(2\mathbf{v}^f + \mathbf{v}^m)\left(3\mathbf{v}^m - 3\mathbf{v}^f + 4(\mathbf{v}^f)^2\right)\right]\right\}}{-k^m\mathbf{v}^f(\mathbf{v}^m + 2\mathbf{v}^f) + k^f[\mathbf{v}^f(5\mathbf{v}^f + 4\mathbf{v}^m) - 3]}$
G	$G^L = \frac{G^m\left[G^m(\mathbf{v}^m)(7\mathbf{v}^f + 2\mathbf{v}^m) + G^f(8 + 7\mathbf{v}^f - 5(2 + \nu_f)\nu_m)\right]}{2G^f(\mathbf{v}^m)(\mathbf{v}^m - 4\mathbf{v}^f) + G^m(-7\mathbf{v}^f - 2\mathbf{v}^m + 2\mathbf{v}^f(\mathbf{v}^m - 4\mathbf{v}^f))}$	$G^U = \frac{G^f\left[G^f\mathbf{v}^f(7\mathbf{v}^m - 2\mathbf{v}^f) + G^m(15 + 7\mathbf{v}^f(5\mathbf{v}^f - 22))\right]}{2G^m\mathbf{v}^f(4\mathbf{v}^m - \mathbf{v}^f) + G^f(15 + \mathbf{v}^f(10\mathbf{v}^f - 23))}$
E	$E^L = \frac{9k^LG^L}{3k^L + G^L}$	$E^U = \frac{9k^UG^U}{3k^U + G^U}$
ν	$\nu^L = \frac{3k^L - 2G^L}{2(3k^L + G^L)}$	$\nu^U = \frac{3k^U - 2G^U}{2(3k^U + G^U)}$

Superscripts "L" and "U" indicate lower and upper bounds, respectively, for corresponding physical properties. Superscripts "f" and "m" indicate filler and matrix phases, respectively. Physical properties of filler phase are assumed to be superior to those of the matrix phase. All formulae adapted from Ref. [76].

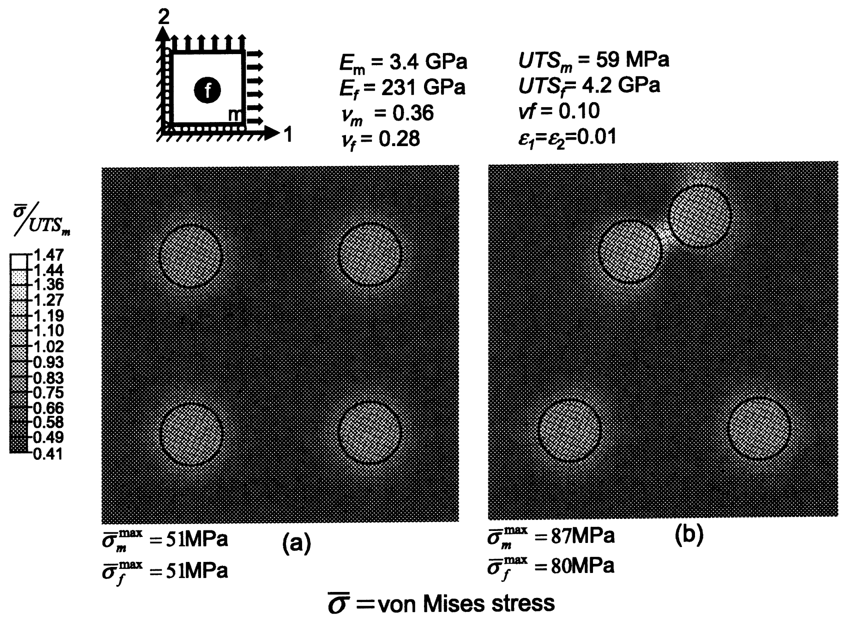

Fig. 8 2D models of transverse stress distributions in an elastic, carbon-epoxy, fiber-reinforced composites. For the simulations shown, $E_f = 231$GPa, $E_m = 3.4$ GPa, $\nu_f = 0.28$, $\nu_m = 0.36$ and $Vf = 0.1$; both simulations are subjected to a biaxial tension of 1%, resulting in far field von Mises stresses of 26 MPa. In the regular array (a), the highest stress is 51MPa at both matrix and fiber phases, whereas in the disordered array (b), the highest stresses are 87 MPa in matrix phase and 80 MPa in fiber phases between the closely-spaced fibers. Material constants for AS4C Hexel® Carbon fibers were obtained from Ref. [77,78]. Material constants for Hercules 3501-6 epoxy were obtained from Ref. [6,79].

Later, Budansky extended their work in order to determine bounds on shear and bulk moduli of multiphase materials.[37] Hashin and Shtrikman used a variational method to minimize potential energy in a model domain and provide rigorous bounds on effective magnetic permeability, shear, and bulk moduli of multiphase materials.[32,73–75] Christensen and Lo later devised a three-phase self-consistent approach to calculate effective shear moduli of materials containing spherical and cylindrical inclusions.[46]

Importantly, many classical results for effective conductivity and effective bulk modulus coincide for both physical and self-consistent RVEs. Effective elastic properties can be found for these arrangements via minimization of potential energy, or minimization or work principles, expressing stored elastic energy as either

$$U_C = \frac{1}{2}\sum_{i=1}^{6}\sum_{j=1}^{6}\varepsilon_i C_{ij}\varepsilon_j \tag{29}$$

or

$$U_S = \frac{1}{2}\sum_{i=1}^{6}\sum_{j=1}^{6}\sigma_i (S_{ij}/m_i m_j)\sigma_j \tag{30}$$

These two expressions result in different magnitudes for the total stored elastic energy in heterogeneous domains due to simplifying assumptions regarding stress and strain fields. Together, they allow calculation of bounds on properties of anisotropic fields of fibrous (Table 5) and particulate (Table 6) materials, with assumed geometry and volume fraction of phases (summarized in compact form, for example, by McCullough,[76] following work by Hashin and Shtrikman[74,75]). These estimates are useful for design for stiffness, in both fibrous and particulate materials, and can be readily used to model a wide range of materials, and compare well with elastic finite element simulations in prediction of stiffnesses[67] we note that these models assume transverse isotropy in the composite, with isotropic fiber and matrix.

Though effective properties can be estimated and bounded using these simplified elastic estimates, however, the importance of disorder in material geometry at the scale at which the material is used must frequently be considered. Such disorder can create internal nonuniformities in material response, and thus variability among devices or structures created from the material. Also, variability in location of reinforcement phases can result in higher stress concentrations in the material, producing earlier-than-expected failure (Fig. 8[77–79]).

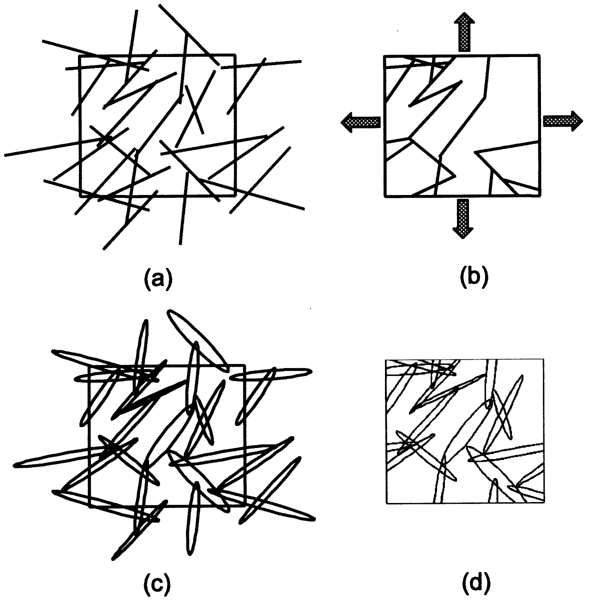

Fig. 9 Micromechanical models of disordered composite materials, including disordered 1D fibrous inclusions, with (a) randomly-laid, and (b) reduced, and periodic geometry, and 2D, fibrous or particulate inclusions, with (c) randomly-laid and (b) reduced, and periodic geometry.

Indeed, real, disordered, or stochastic materials exhibit a range of values in material response, and attempts have been made for various geometries (e.g., randomly laid fibers or particles, as in Fig. 9) to bound these properties. Work of this type models disorder in a material specifically, rather than through use of an energy approach, as described in the previous section, to simply bound properties of an ordered, representative arrangement. In early work, Bergman devised an analytical method to determine bounds for dielectric conductivity[80] Lurie and Cherkaev[81] and Milton and Kohn[82] presented bounds for macroscopically aniotropic media by extending the work of Hashin and Shtrikman.[32,73,74] Gibiansky and Torquato used a ''translation method'' to determine the rigorous bounds for the relation between conductivity and elastic moduli of two-dimensional, globally isotropic composite materials.[83] Later, Torquato and coworkers used a discrete network and homogenization theory to determine the effective mechanical and transport properties of cellular solids.[84] Studying fibrous materials, Lu, Carlsson, and Andersson used a micromechanical approach to obtain rigorous bounds on elastic properties.[85–87] And Ostoja-Starzewski et al. developed network techniques to simulate effective properties of generalized composites by changing the spring constants of individual springs within the network to model multiphase material properties.[88] Sastry and coworkers studied the stochastic fibrous networks to determine both conductivity and variance in conductivity in battery materials.[89,90] This work was later extended to model fiber type bonding conditions, and failure mechanisms in greater detail[90,91] and was also extended to include the effects of fiber waviness on material mechanical properties[92–94] to model variance in electrical conductivity of porous networks with elliptical particles.[95]

PHASE CONTINUITY AND PERCOLATION IN DISORDERED COMPOSITES

All of these efforts further underscored the importance of variance in properties in real materials. Indeed, a key requirement in producing dramatic changes in material transport properties (e.g., thermal and electrical conduction) is percolation of the additive phase. We can define percolation as the formation of at least one, continuous, domain-spanning path of the percolating phase in the material. Dramatic improvements in computing speeds from the 1980s to the present have allowed direct, stochastic simulation of transport in disordered arrays.

Key features of such models include physically realistic simulation domains and use of many statistically equivalent realizations, i.e., domains in which the statistical parameters describing particles, sizes, etc. are the same for all, but the locations, sizes, etc. are different in each. As a result, the minimum amount of a phase required to produce dramatic improvements in composite properties can be determined, along with discrete and averaged predictions of material properties. Percolation concepts have been used not only in design of materials for mechanical[96–98] properties, but also in filtration[99–101] and conductive[89–103] properties.

Classic work by Kirkpatrick, who studied site and bond percolation using a resistor network, pointed out the importance of the percolation threshold, or threshold

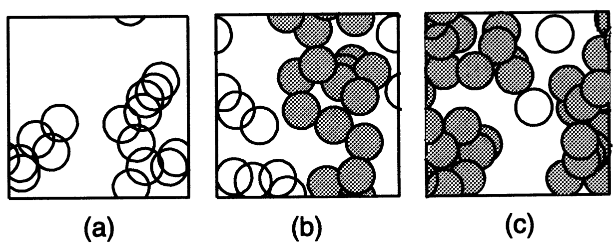

Fig. 10 Percolating and non-percolating arrays of circles, with volume fractions (a) 32.7%, (b) 51.2%, and (c) 64.0%.

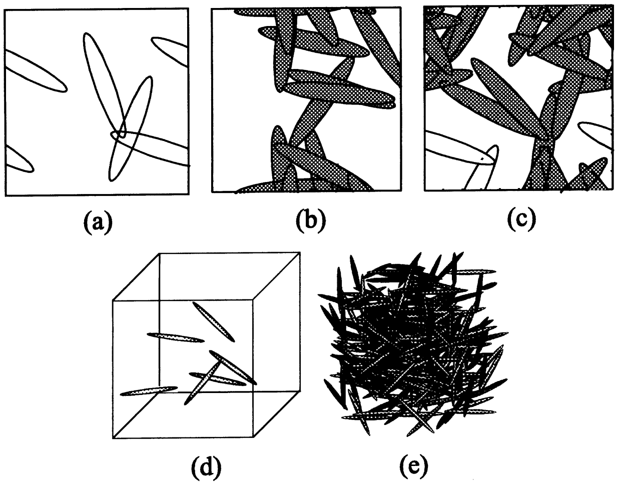

Fig. 11 Two-dimensional percolating and nonpercolating arrays of ellipses of aspect ratio 6 and volume fractions (a) 17.9%, (b) 31.6%, and (c) 50.7%. Three-dimensional percolating and nonpercolating arrays of ellipsoids are also shown, of aspect ratio 10, and volume fraction (d) 6%, and (e) 20%.

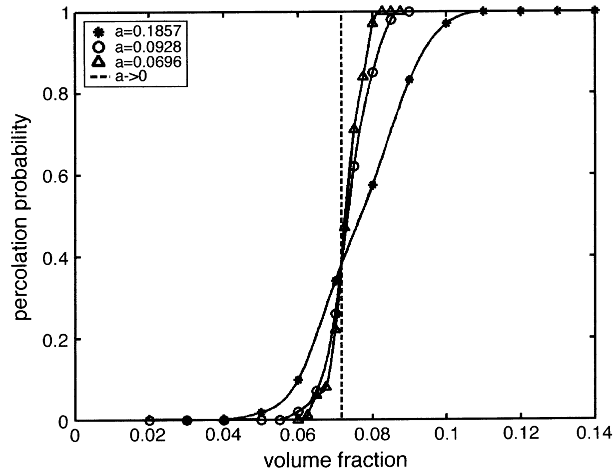

Fig. 13 Simulation results for percolation probability versus particle size, for arrays of overlapping ellipsoids of revolution. In this figure, 'a' represents the semi-axis length, and the aspect ratio of the ellipsoids is 10. (Adapted from Ref. [107].)

volume fraction above which a percolating phase would form at least one single, domain-spanning path (Fig. 10).[104] In 1988, McLachlan introduced a more general effective-media equation for binary conductivity media.[47] The fact that higher aspect ratio phases percolate at lower volume or area fractions than lower aspect ratio phases has been well documented. In early work, Kirkpatrick's simulations showed that the percolation threshold ρ_c, i.e., the density or volume fraction of the fiber phases at percolation onset, exhibited a power law dependence upon bond fraction v.[104] Pike and Seager also examined conduction and percolation phenomena in stick networks (among others), using 2-D and 3-D Monte Carlo simulations.[105]

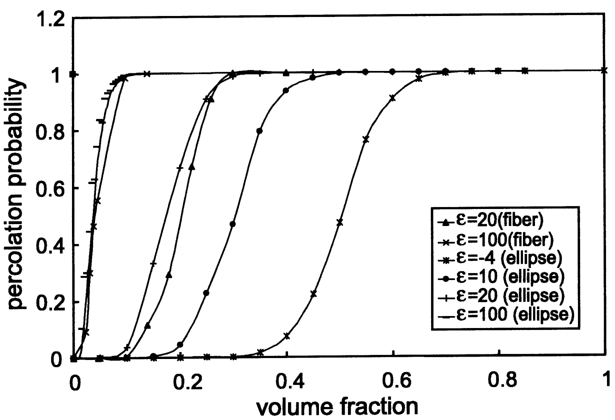

Fig. 12 Probability of percolation in 2D arrays, for various particle-fiber geometrics. (Adapted from Ref. [106].)

Recently, analytical approximations of the percolation points have been developed for both 2-D and 3-D arrays of generalized ellipses and ellipsoids of uniform shape and size,[106,107] which verified and extended earlier results on simulation of simpler 2-D networks of 1-D fiber percolation,[97,98] 3-D networks of 2-D ellipsoids, and other analytical approaches for determination of percolation of circular arrays;[108–114] combined results[91,106] are shown in Fig. 11. These illustrate that the percolation point in realistic materials is probabilistic (i.e., only a statistical estimation of percolation point can be made, for any given volume fraction of particles), and also that 2-D fiber models in models are quite satisfactory for determining percolation properties for aspect ratios greater than 100, as shown in Fig. 12. Similarly, Fig. 13 shows that percolation probability of ellipsoid models in 3-D model is also strongly dependent upon of aspect ratio.

APPLICATION OF COMPOSITE THEORIES TO BIOMATERIALS

Modeling of the shapes and effects of various phases in materials is tremendously important in understanding the combined mechanical and physiological role of biomaterials. Natural materials exhibit a high degree of variability, and use of statistical theories touched upon in this chapter can be helpful in anticipating differences in clinical results of both in-vitro and in-vivo tissue response. Generalized domains, particularly fields of ellipses and ellipsoidal particles, can be used to describe a wide variety of materials and bound a number of important effective engineering properties. Percolative properties have important implications for understanding the role of particulates (either voids or material phases) and fibers, both adaptation and selection, in biomaterials (Fig. 12).

Thus, in conclusion, the modeling of heterogeneous domains performed by the composites community has broad application in modeling biomaterials. Elasticity provides an initial estimate of properties, and percolation theories provide a method of determining the connectivity of phases, and thus their importance in transport.

ACKNOWLEDGMENTS

The authors wish to acknowledge the invaluable assistance of Dr. Yun-Bo Yi, Dr. Bradley Layton, Dr. Hui Wang, and Dr. Scott Hollister, who provided simulation data and/or images for this chapter, and of Mr. Taeyong Kim, in helping to collect materials.

ARTICLES OF FURTHER INTEREST

Alumina, p. 19
Degradable Polymer Composites, p. 423
Finite Element Analysis, p. 621

REFERENCES

1. Christensen, R.M. *Mechanics of Composite Materials*; John Wiley and Sons: New York, 1979.
2. Carlsson, L.A.; Pipes, R.B. *Experimental Characterization of Advanced Composite Materials*; Prentice-Hall: Englewood Cliffs, NJ, 1987.
3. Vinson, J.R. *The Behavior of Sandwich Structures of Isotropic and Composite Materials*; Technomic Pub. Co.: Lancaster, PA, 1999.
4. Carlsson, L.A.; Gillespie, J.W.; Zweben, C.H. *Delaware Composites Design Encyclopedia*; Technomic Pub. Co.: Lancaster, PA, 1989.
5. Chou, T.-W. *Microstructural Design of Fiber Composites*; Cambridge University Press: Cambridge, 1992.
6. Gutowski, T.G.P. *Advanced Composites Manufacturing*; John Wiley & Sons: New York, 1997.
7. Taboas, J.M.; Maddox, R.D.; Krebsbach, P.H.; Hollister, S.J. Indirect solid free form fabrication of local and global porous, biomimetic and composite 3d polymer-ceramic scaffolds. Biomaterials **2003**, *24* (1), 181–194.
8. Kimball, J.W. *Biology*, 2nd Ed.; Addison-Wesley Pub. Co.: Reading, MA, 1968.
9. Rubin, G.M.; Yandell, M.D.; Wortman, J.R.; Miklos, G.L.G.; Nelson, C.R.; Hariharan, I.K.; Fortini, M.E.; Li, P.W.; Apweiler, R.; Fleischmann, W.; Cherry, J.M.; Henikoff, S.; Skupski, M.P.; Misra, S.; Ashburner, M.; Birney, E.; Boguski, M.S.; Brody, T.; Brokstein, P.; Celniker, S.E.; Chervitz, S.A.; Coates, D.; Cravchik, A.; Gabrielian, A.; Galle, R.F.; Gelbart, W.M.; George, R.A.; Goldstein, L.S.B.; Gong, F.C.; Guan, P.; Harris, N.L.; Hay, B.A.; Hoskins, R.A.; Li, J.Y.; Li, Z.Y.; Hynes, R.O.; Jones, S.J.M.; Kuehl, P.M.; Lemaitre, B.; Littleton, J.T.; Morrison, D.K.; Mungall, C.; O'farrell, P.H.; Pickeral, O.K.; Shue, C.; Vosshall, L.B.; Zhang, J.; Zhao, Q.; Zheng, X.Q.H.; Zhong, F.; Zhong, W.Y.; Gibbs, R.; Venter, J.C.; Adams, M.D.; Lewis, S. Comparative genomics of the eukaryotes. Science **2000**, *287* (5461), 2204–2215.
10. Mossotti, O.F. Memorie di Matematica e Fisica della Societa Italiana delle Scienze. **1850**, *24*, 49.
11. Clausius, R. Die mechanische warmetheorie II. Braunschweig **1879**, *62*.
12. Lorenz, L.V. Ann. Phys. **1880**, *11*, 70.
13. Lorentz, H.A. Ann. Phys. **1880**, *9*, 641.
14. Maxwell, J.C.A. *Treatise on Electricity and Magnetism*; Dover: New York, 1891.
15. Rayleigh, L.J.W. On the influence of obstacles arranged in rectangular order upon the properties of a medium. Philos. Mag. Ser. **1892**, *5* (34), 481–502.
16. Einstein, A. Eine neue bestimmung der molekuldimensionen. Ann. Phys. **1906**, *19*, 289.
17. Wiener, O. Die theorie des mischkörpers für das feld des stationaren strömung. Abh. Math.-Phys. Kl. Königl. Sächs. Gesel. Wissen. **1912**, *32*, 509–604.
18. Fricke, H. Phys. Rev. **1924**, *24*, 575.
19. Lichtenecker, K. Phys. Z. **1926**, *27*, 115.
20. Runge, I.Z. Teck. Phys. **1925**, *6*, 61.
21. Goodier, J.N. Concentration of stress around spherical and cylindrical inclusion and flaws. J. Appl. Mech. **1933**, *55*, 39–44.
22. Bruggeman, D.A.G. Berechnung verschiedener physikalischer konstanten von heterogenen substanzen: I. Dielektrizitatskonstanten und leifahigkeiten der mischkorper aus isotropen substanzen. Ann. Phys. **1935**, *24* (5), 636–679.
23. Dewey, J.M. The elastic constants of materials loaded with non-rigid fillers. J. Appl. Phys. **1947**, *18* (6), 578–581.
24. Landauer, R. The electrical resistance of binary metallic mixtures. J. Appl. Phys. **1952**, *23* (7), 779–784.
25. Hershey, A.V. The elasticity of an isotropic aggregate of anisotropic cubic crystals. J. Appl. Mech., Trans. ASME **1954**, *21* (3), 236–240.
26. Brown, W.F. Solid mixture permittivities. J. Chem. Phys. **1955**, *23* (8), 1514–1517.

27. Eshelby, J.D. The determination of the elastic field of an ellipsoidal inclusion, and related problems. Proc. R. Soc. Lond., A Math. Phys. Sci. **1957**, *241* (1226), 376–396.
28. Kerner, E.H. The electrical conductivity of composite media. Proc. Phys. Soc. Lond., B **1956**, *69* (8), 802–807.
29. Van Der Pol, C. On the rheology of concentrated dispersions. Rheol. Acta **1958**, *1*, 198.
30. Meredith, R.E.; Tobias, C.W. Resistance to potential flow through a cubical array of spheres. J. Appl. Phys. **1960**, *31* (7), 1270–1273.
31. Hashin, Z. The elastic moduli of heterogeneous materials. J. Appl. Mech., Trans. ASME **1962**, *29* (3), 143–150.
32. Hashin, Z.; Shtrikman, S. A variational approach to the theory of the elastic behaviour of polycrystals. J. Mech. Phys. Solids **1962**, *10* (4), 343–352.
33. Keller, J.B. Theorem on conductivity of composite medium. J. Math. Phys. **1964**, *5* (4), 548.
34. Hashin, Z.; Rosen, B.W. The elastic moduli of fiber-reinforced materials. J. Appl. Mech., Trans. ASME **1964**, *31*, 233.
35. Hill, R. Theory of mechanical properties of fibre-strengthened materials. 1. Elastic behaviour. J. Mech. Phys. Solids **1964**, *12* (4), 199–212.
36. Hill, R. A self-consistent mechanics of composite materials. J. Mech. Phys. Solids **1965**, *13* (4), 213.
37. Budiansk, B. On elastic moduli of some heterogeneous materials. J. Mech. Phys. Solids **1965**, *13* (4), 223.
38. Hashin, Z. Viscoelastic fiber reinforced materials. AIAA J. **1966**, *4* (8), 1411.
39. Russel, W.B.; Acrivos, A. Effective moduli of composite-materials—Slender rigid inclusions at dilute concentrations. Zeit. Angew. Math. Phys. **1972**, *23* (3), 434–463.
40. Russel, W.B. Effective moduli of composite-materials—Effect of fiber length and geometry at dilute concentrations. Zeit. Angew. Math. Phys. **1973**, *24* (4), 581–600.
41. Mendelson, K.S. Theorem on effective conductivity of a two-dimensional heterogeneous medium. J. Appl. Phys. **1975**, *46* (11), 4740–4741.
42. Doyle, W.T. Clausius-mossotti problem for cubic arrays of spheres. J. Appl. Phys. **1978**, *49* (2), 795–797.
43. Mcphedran, R.C.; Mckenzie, D.R. Conductivity of lattices of spheres. 1. Simple cubic lattice. Proc. R. Soc. Lond., A Math. Phys. Eng. Sci. **1978**, *359* (1696), 45–63.
44. Landauer, R. Stability in dissipative steady-state. Phys. Today **1978**, *31* (11), 23–29.
45. Perrins, W.T.; Mckenzie, D.R.; Mcphedran, R.C. Transport-properties of regular arrays of cylinders. Proc. R. Soc. Lond., A Math. Phys. Eng. Sci. **1979**, *369* (1737), 207–225.
46. Christensen, R.M.; Lo, K.H. Solutions for effective shear properties in 3 phase sphere and cylinder models. J. Mech. Phys. Solids **1979**, *27* (4), 315–330.
47. Mclachlan, D.S. Measurement and analysis of a model dual-conductivity medium using a generalized effective-medium theory. J. Phys. C. Solid State Phys. **1988**, *21* (8), 1521–1532.
48. Bao, K.D.; Axell, J.; Grimvall, G. Electrical-conduction in checkerboard geometries. Phys. Rev., B **1990**, *41* (7), 4330–4333.
49. Guedes, J.M.; Kikuchi, N. Preprocessing and postprocessing for materials based on the homogenization method with adaptive finite-element methods. Comput. Methods Appl. Mech. Eng. **1990**, *83* (2), 143–198.
50. Gu, G.Q.; Liu, Z.R. Thermal-conductivity of periodic composite media with spherical inclusions. Commun. Theor. Phys. **1991**, *15* (2), 141–148.
51. Gu, G.Q. Calculation methods for effective constants of periodic composite media. J. Phys., D. Appl. Phys. **1993**, *26* (9), 1371–1377.
52. Christensen, R.M. Effective properties of composite-materials containing voids. Proc. R. Soc. Lond., A Math. Phys. Eng. Sci. **1993**, *440* (1909), 461–473.
53. Lu, S.Y. The effective thermal-conductivities of composites with 2-d arrays of circular and square cylinders. J. Compos. Mater. **1995**, *29* (4), 483–506.
54. Batchelor, G.K. Transport properties of 2-phase materials with random structure. Annu. Rev. Fluid Mech. **1974**, *6*, 227–255.
55. Whitney, J.M.; Mccullough, R.L. Micro-Models for Predicting Viscoelastic Behavior. In *Delaware Composites Design Encyclopedia*; Whitney, J.M., Mccullough, R.L., Eds.; Technomic Pub. Co.: Lancaster, PA, USA, 1990; Vol. 2, 189–201.
56. Sastry, A.M. 2.17 Impregnation and Consolidation Phenomena. In *Comprehensive Composite Materials*; Kelly, A., Zweben, C.H., Eds.; Elsevier: Amsterdam, 2000; Vol. II, 609–622.
57. Fung, Y.C. *Introduction to Bioengineering*; World Scientific: Singapore, 2001.
58. Torquato, S. *Random Heterogeneous Materials: Microstructure and Macroscopic Properties*; Springer: New York, 2002.
59. Tsai, S.W.; Wu, E.M. General theory of strength for anisotropic materials. J. Compos. Mater. **1971**, *5*, 58. (JAN).
60. Tsai, S.W.; Hahn, H.T. *Introduction to Composite Materials*; Technomic Pub. Co.: Westport, CT, 1980.
61. Sastry, A.M.; Phoenix, S.L. Load redistribution near nonaligned fiber breaks in a 2-dimensional unidirectional composite using break-influence superposition. J. Mater. Sci. Lett. **1993**, *12* (20), 1596–1599.
62. Sastry, A.M.; Phoenix, S.L.; Schwartz, P. Analysis of interfacial failure in a composite microbundle pull-out experiment. Compos. Sci. Technol. **1993**, *48* (1–4), 237–251.
63. Sastry, A.M.; Phoenix, S.L. Shielding and magnification of loads in elastic, unidirectional composites. SAMPE J. **1994**, *30* (4), 61–67.
64. Beyerlein, I.J.; Phoenix, S.L.; Sastry, A.M. Comparison

of shear-lag theory and continuum fracture mechanics for modeling fiber and matrix stresses in an elastic cracked composite lamina. Int. J. Solids Struct. **1996**, *33* (18), 2543–2574.
65. Phoenix, S.L. Statistical Strength Theory for Fibrous Composite Materials. In *Comprehensive Composite Materials*; Kelly, A., Zweben, C.H., Eds.; Elsevier: Amsterdam, 2000; Vol. I, 559.
66. Reddy, J.N. *Mechanics of Laminated Composite Plates: Theory and Analysis*; CRC Press: Boca Raton, 1997.
67. Hyer, M.W. *Stress Analysis of Fiber-Reinforced Materials*; WCB McGraw-Hill: Boston, 1998. Especially Chapter 3.
68. Reuss, A. Berechnung der fliessgrenze kristallen von mischkristallen auf grund der plastizitatsbedingung fur einkristalle. Math. Mech. Z. Angew. **1929**, *9*, 49.
69. Voigt, W. *Lehrbuch der Kristallphysik*; B.G. Teubner: Leipzig, 1910.
70. Boucher, S. On the effective moduli of isotropic two-phase elastic composites. J. Compos. Mater. **1974**, *8* (82).
71. Hershey, A.V. The plasticity of an isotropic aggregate of anisotropic face-centered cubic crystals. J. Appl. Mech., Trans. ASME **1954**, *21* (3), 241–249.
72. Kröner, E. Berechnung der elastischen konstanten des vielkristalls aus den konstanten des einkristalls. Zeit. Phys. **1958**, *151* (4), 504–518.
73. Hashin, Z.; Shtrikman, S. A variational approach to theory of effective magnetic permeability of multiphase materials. J. Appl. Phys. **1962**, *33* (10), 3125.
74. Hashin, Z.; Shtrikman, S. On some variational principles in anisotropic and nonhomogeneous elasticity. J. Mech. Phys. Solids **1962**, *10* (4), 335–342.
75. Hashin, Z.; Shtrikman, S. A variational approach to the theory of the elastic behaviour of multiphase materials. J. Mech. Phys. Solids **1963**, *11* (2), 127–140.
76. Mccullough, R.L. Micro-Models for Composite Materials. In *Delaware Composites Design Encyclopedia*; Whitney, J.M., Mccullough, R.L., Eds.; Technomic Pub. Co.: Lancaster, PA, USA, 1990; *2*, 49–142.
77. http://www.matweb.com (2003).
78. Kriz, R.D.; Stinchcomb, W.W. Elastic-moduli of transversely isotropic graphite fibers and their composites. Exp. Mech. **1979**, *19* (2), 41–49.
79. http://structures.ucsd.edu (2003).
80. Bergman, D.J. Analytical properties of the complex effective dielectric constant of a composite medium with applications to the derviation of rigrous bounds and to percolation problems.
81. Lurie, K.A.; Cherkaev, A.V. Exact estimates of conductivity of composites formed by 2 isotropically conducting media taken in prescribed proportion. Proc. R. Soc. Edinb., Sect. A, Math. **1984**, *99*, 71–87.
82. Milton, G.W.; Kohn, R.V. Variational bounds on the effective moduli of anisotropic composites. J. Mech. Phys. Solids **1988**, *36* (6), 597–629.
83. Gibıansky, L.V.; Torquato, S. Link between the conductivity and elastic-moduli of composite-materials. Phys. Rev. Lett. **1993**, *71* (18), 2927–2930.
84. Torquato, S.; Gibiansky, L.V.; Silva, M.J.; Gibson, L.J. Effective mechanical and transport properties of cellular solids. Int. J. Mech. Sci. **1998**, *40* (1), 71–82.
85. Lu, W.T.; Carlsson, L.A.; Andersson, Y. Micro model of paper. 1. Bounds on elastic properties. Tappi J. **1995**, *78* (12), 155–164.
86. Lu, W.T.; Carlsson, L.A. Micro-model of paper. 2. Statistical analysis of the paper structure. Tappi J. **1996**, *79* (1), 203–210.
87. Lu, W.T.; Carlsson, L.A. Influence of viscoelastic behavior on curl of paper. Mech. Time-Depend. Mater. **2001**, *5* (1), 79–100.
88. Ostoja-Starzewski, M.; Sheng, P.Y.; Jasiuk, I. Damage patterns and constitutive response of random matrix-inclusion composites. Eng. Fract. Mech. **1997**, *58* (5–6), 581–606.
89. Cheng, X.; Sastry, A.M. On transport in stochastic, heterogeneous fibrous domains. Mech. Mater. **1999**, *31* (12), 765–786.
90. Wang, C.W.; Berhan, L.; Sastry, A.M. Structure, mechanics and failure of stochastic fibrous networks: Part I—Microscale considerations. J. Eng. Mater. Technol. Trans. ASME **2000**, *122* (4), 450–459.
91. Wang, C.W.; Sastry, A.M. Structure, mechanics and failure of stochastic fibrous networks: Part II—Network simulations and application. J. Eng. Mater. Technol. Trans. ASME **2000**, *122* (4), 460–468.
92. Berhan, L.; Yi, Y.B.; Sastry, A.M. Effect of nanorope waviness on the effective moduli of nanotube sheets. J. Appl. Phys. **2004**, *95* (8), 4335–4345.
93. Berhan, L.; Yi, Y.B.; Sastry, A.M.; Munoz, E.; Selvidege, M.; Baughman, R. Mechanical properties of nanotube sheets: Alteration in joint morphology, and achievable moduli in manufacturable materials. J. Appl. Phys. **2004**, *95* (9), 5027–5034.
94. Yi, Y.B.; Berhan, L.; Sastry, A.M. Statistical geometry of random fibrous networks, revisited: Waviness, dimensionality and percolation. J. Appl. Phys. **2004**. Accepted.
95. Wang, C.W.; Cook, K.A.; Sastry, A.M. Conduction in multiphase particulate/fibrous networks simulations and experiments on li-ion anodes. J. Electrochem. Soc. **2003**, *150* (3), A385–A397.
96. Sastry, A.M.; Cheng, X.; Wang, C.W. Mechanics of stochastic fibrous networks. J. Thermoplast. Compos. Mater. **1998**, *11* (3), 288–296.
97. Cheng, X.; Wang, C.W.; Sastry, A.M.; Choi, S.B. Investigation of failure processes in porous battery substrates: Part II—Simulation results and comparisons. J. Eng. Mater. Technol. Trans. ASME **1999**, *121* (4), 514–523.
98. Wang, C.W.; Cheng, X.; Sastry, A.M.; Choi, S.B. Investigation of failure processes in porous battery substrates: Part I—Experimental findings. J. Eng.

Mater. Technol. Trans. ASME **1999**, *121* (4), 503–513.

99. Nielaba, P.; Privman, V. Multilayer adsorption with increasing layer coverage. Phys. Rev., A **1992**, *45* (8), 6099–6102.
100. Deckmyn, P.; Davies, G.A.; Bell, D.J. Properties of percolating clusters on finite lattices applied to model filtration processes. Appl. Math. Model. **1995**, *19* (5), 258–269.
101. Datta, S.; Redner, S. Gradient and percolative clogging in depth filtration. Int. J. Mod. Phys. C **1998**, *9* (8), 1535–1543.
102. Cheng, X.; Sastry, A.M.; Layton, B.E. Transport in stochastic fibrous networks. J. Eng. Mater. Technol. Trans. ASME **2001**, *123* (1), 12–19.
103. Mohanty, S.; Sharma, M.M. A Monte-Carlo RSRG method for the percolation conduction properties of correlated lattices. Phys. Lett., A **1991**, *154* (9), 475–481.
104. Kirkpatrick, S. Percolation and conduction. Rev. Mod. Phys. **1973**, *45* (4), 574–588.
105. Pike, G.E.; Seager, C.H. Percolation and conductivity—Computer study. 1. Phys. Rev., B **1974**, *10* (4), 1421–1434.
106. Yi, Y.B.; Sastry, A.M. Analytical approximation of the two-dimensional percolation threshold for fields of overlapping ellipses. Phys. Rev., E **2002**, *66* (6). Art. no.-066130.
107. Yi, Y.B.; Sastry, A.M. Analytical approximation of the percolation threshold for overlapping ellipsoids of revolution. Proc. R. Soc. Lond., A **2004**, accepted.
108. Haan, S.W.; Zwanzig, R. Series expansions in a continuum percolation problem. J. Phys., A, Math. Gen. **1977**, *10* (9), 1547–1555.
109. Coniglio, A.; Deangelis, U.; Forlani, A.; Lauro, G. Distribution of physical clusters. J. Phys., A, Math. Gen. **1977**, *10* (2), 219–228.
110. Coniglio, A.; Deangelis, U.; Forlani, A. Pair connectedness and cluster size. J. Phys., A, Math. Gen. **1977**, *10* (7), 1123–1139.
111. Hill, T.L. Molecular clusters in imperfect gases. J. Chem. Phys. **1955**, *23* (4), 617–622.
112. Drory, A. Theory of continuum percolation. I. General formalism. Phys. Rev., E **1996**, *54* (6), 5992–6002.
113. Quintanilla, J.; Torquato, S. Clustering properties of d-dimensional overlapping spheres. Phys. Rev., E **1996**, *54* (5), 5331–5339.
114. Quintanilla, J.; Torquato, S. Clustering in a continuum percolation model. Adv. Appl. Probab. **1997**, *29* (2), 327–336.